Advanced Electron Linacs

R. H. Siemann*

Stanford Linear Accelerator Center, Stanford University, Stanford, CA 94309 USA

ABSTRACT

The research into advanced acceleration concepts for electron linear accelerators being pursued at SLAC is reviewed. This research includes experiments in laser acceleration, plasma wakefield acceleration, and mm-wavelength RF driven accelerators.

I. INTRODUCTION

The frontier of particle physics is determined by the highest achievable center-of-mass energy. There has been exponential growth in center-of-mass energy because of *i)* conceptual breakthroughs in acceleration (for example, strong focusing and colliding beams); *ii)* inventions such as the klystron; *iii)* application of technologies like superconductivity to particle acceleration; and *iv)* consolidation of high energy physics research at fewer and larger facilities.

The latter is a trend that cannot go much farther for reasons that include but go even beyond the political vulnerability of large accelerator complexes. High energy physics experiments performed by a thousand or more scientists at remote sites are not in a strong competitive position for university positions and for the ambitious young people who want to tackle and solve important problems. Already one sees talented particle physicists performing research that is on the fringes of traditional high energy physics. Particle physics evolving as it is now will be addressing some of the most questions posed by mankind, but in a manner and at a cost that possibly cannot be sustained.

Such extrapolations into the future ignore the possibility of revolutionary developments. These could be particle physics discoveries or accelerator inventions that dramatically reduce costs and increase capabilities. The accelerator research described in this paper is one attempt to pose and answer questions that could lead to inventions and dramatic changes in electron linear accelerators.

At the present time this research is concentrated on three questions:

- Lasers are capable of terawatts of peak power. What is the potential of lasers as an accelerator power source?
- Laser driven, plasma based accelerators have demonstrated gradients of 100 GV/m. What is the next step in the development of plasma based accelerators?
- RF driven accelerators can have an acceleration gradient that is roughly proportional to frequency. What are the limits of high frequency accelerators?

* Work supported by the Department of Energy, contract DE-AC03-76SF00515.

II. LASER ACCELERATION

Laser irradiance as high 10^{19} W/cm^2 corresponding to electric fields of 10 GV/m has been achieved on existing multi-terawatt systems.[1] Solid state diode pumped lasers have good efficiency, the promise of high average power, and market forces driving development. With these attributes the laser is natural for acceleration, but the electric field is transverse to the direction of propagation. There are a number of possible ways to remove this restriction:

- The electron beam in an Inverse Free Electron Laser has a wiggle component of motion transverse to the average propagation direction, but synchrotron radiation in the wiggler magnets limits the energy.
- Laser excited plasma space charge waves have reached gradients of 100 GV/m. There is more on plasma acceleration in section III below.
- A structure with feature sizes the order of a wavelength, as in RF accelerators, would have enormous wakefields and small accelerated charge. A structure with features much larger than the wavelength does not have as severe wakefields and could accelerate higher charge.

This is the underpinning of the crossed laser beam accelerator illustrated in Figure 1.[2] Two laser beams, formed by splitting a single beam, are crossed at an angle θ. The beams are polarized in the crossing plane, and the

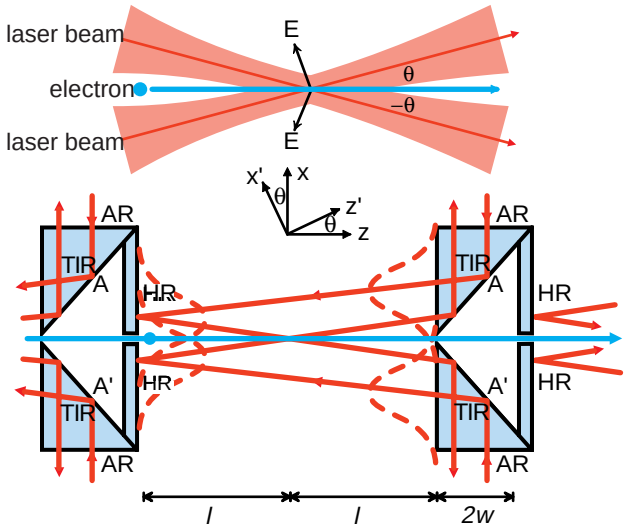

Figure 1: Schematic of a crossed laser beam accelerator.[2] The beams are focused to a waist in the middle of the structure. AR, HR, and TIR denote anti-reflection coating, high reflectively coating, and total internal reflection, respectively. Acceleration takes place over the length 2l between slits.

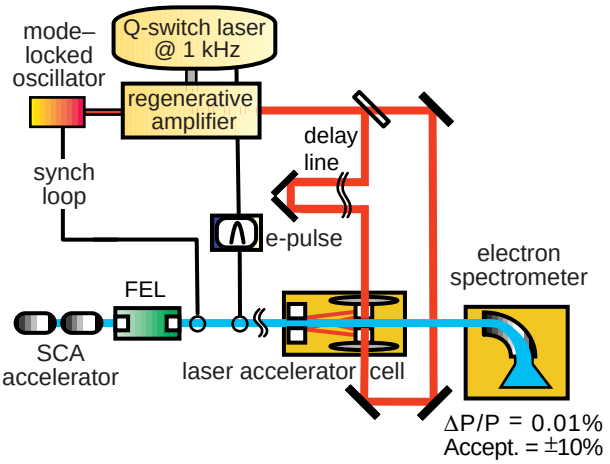

Figure 2: Schematic of structure based laser acceleration experiment.

optical path lengths are such that the transverse components of electric field interfere destructively and the longitudinal components add constructively.

Treating the laser beams as focused, free space Gaussian beams,[3] the on-axis, longitudinal electric field in terms of the laser power, P, the wave impedance of free space η_v, the waist size, w_0, and the Rayleigh range, $z_r = \pi w_0^2/\lambda$, is

$$E_z = -\sqrt{\frac{\eta_v P}{\pi}}\,\frac{4\theta}{w_0\left(1+(z/z_r)^2\right)}\exp\left(-\frac{z^2\theta^2}{w^2}\right) \times\exp\left(i\left[2\varphi_g+\varphi_r+\varphi_p\right]\right) \quad (1)$$

where

$$w^2 = w_0^2\left(1+\frac{z^2}{z_r^2}\right). \quad (2)$$

The three phases are: the Guoy phase advance that occurs passing through the focus of a beam where the wavefronts change from incoming to outgoing spherical waves (there is a factor of two from summing transverse and longitudinal field components),

$$\tan\varphi_g = z/z_r\ ; \quad (3)$$

the radial phase that accounts for wavefront curvature,

$$\varphi_r = -\frac{z}{z_r}\frac{z^2\theta^2}{w^2}; \quad (4)$$

and the relative phase of a charged particle with respect to the accelerating field

$$\varphi_p = \frac{\pi z}{\lambda}\left(\theta^2-\frac{1}{\gamma^2}\right). \quad (5)$$

For an infinite range of integration, there is no net acceleration due to the phase slip between particles and accelerating field. The field must be terminated with slits at $|z| < z_r$ by a structure for net acceleration. The maximum energy gain of an on-axis electron is

$$\Delta W_{max}(\text{MeV}) = 30\sqrt{P(\text{TW})} \quad (6)$$

with a crossing angle $\theta = 1.37 w_0/z_r$ and an interaction length $2l = 0.92\ z_r$.[2] Average gradients of almost 1 GeV/m are possible without exceeding laser damage thresholds.

The field terminating slits can be at most a few times the laser wavelength in width to avoid substantial loss of acceleration, and, with a bunch length that is a small fraction of the laser wavelength, the longitudinal wakefield in these slits severely limits the accelerated charge. Estimates are that the wakefield energy loss per stage equals the energy gain for ~10^5 electrons. Two solutions of this severe problem have been proposed. First, cylindrical optics and a line charge can be used,[4] and, second, the laser light can be recycled to accelerate multiple beams.[5]

A collaboration between the Ginzton and Hansen Laboratories (HEPL) on the Stanford campus and SLAC are building an experiment to study structure based laser acceleration.[6] The experiment, illustrated in Figure 2 and with parameters given in Table 1, will use a 35 MeV beam from the HEPL superconducting accelerator. A Ti-Sapphire laser and regenerative amplifier will provide the laser light. The electron beam will traverse a Free Electron Laser (FEL) upstream of the laser accelerator, and the Ti-Sapphire laser will be mode locked to the FEL to give picosecond level timing between the laser and beam. A pulsed kicker in the electron beamline downstream of the FEL, triggered in synchronism with the laser Q-switch, will provide low rate beam to the laser accelerator. Emittance filters between the kicker and laser accelerator will control incoming beam intensity and emittance, and the outgoing

Table 1: Laser Acceleration Experiment Parameters

Ti-Saphire Laser Parameters	
Mode lock pulse rate	82 MHz
Regenerative amplifier rate	1 kHz
Energy per pulse	1 mJ
Pulse width	0.1 - 3 psec
Wavelength	0.8 - 1 μm
Superconducting Accelerator (SCA) Parameters	
Micropulse length	2 psec
Electrons per micropulse	10^8
Micropulse rate	11.8 MHz
Macropulse length	2 msec
Macropulse rate	10 Hz
Normalized emittance	8 mm-mrad
RMS energy spread	0.1%
Energy	35 MeV
Laser Acceleration Cell Parameters	
Acceptance	3 mm-mrad
Laser energy per stage	0.1 mJ
Electrons captured	10^7/sec
Energy gain per stage	330 keV

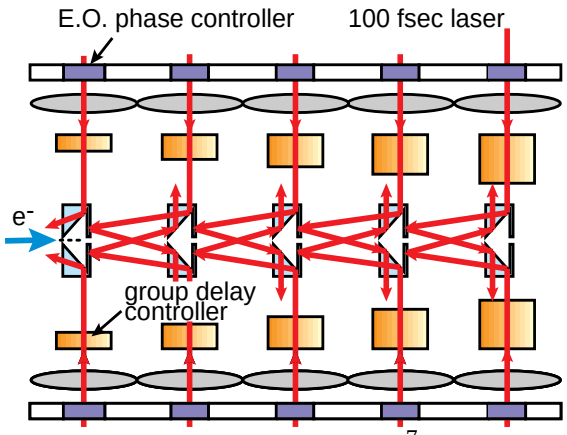

Figure 3: Multi-stage laser acceleration.[7]

beam will be diagnosed with a high resolution spectrometer. Energy gain of 330 keV (~1%) is possible without damaging the laser accelerator optics.

The first experimental run will be in November, 1997 and will be devoted to setting up the laser and electron beam lines and establishing the timing between the two beams. Observation of laser acceleration and measurement of accelerating gradient and beam loading for different accelerator configurations is expected in early 1998. These experiments should establish the viability of this approach to laser acceleration.

Building a high energy linac will require multiple stages for high energy and recycling of the laser light for acceleration of significant charge. One multi-stage concept is illustrated in Figure 3.[7] Light from a multi-terawatt laser is split and drives many cells. There is an overall electro-optical phase control and group delay elements compensate for electron beam transit time. A large accelerator would require many such sections and mode-locking of multiple multi-terawatt lasers. This is still to be accomplished.

The accelerator in Figure 3 has a single electron beam, and longitudinal wakefields could limit the accelerated charge to an unacceptably low value. The "matrix accelerator", proposed by D. Whittum for mm-wave acceleration,[8] recycles the output power that would normally be dumped into a load to accelerate multiple beams that are combined at the end of the accelerator. This seems natural for laser accelerators also. Rather than throwing away the output light in Figure 3 it could be transported to another beamline to accelerate particles there. T. Plettner has devised appropriate optics for this and is studying the wavefronts of the light recycled through multiple stages.[5]

III. PLASMA WAKEFIELD ACCELERATION

Laser or particle beams can excite relativistic plasma waves that have a longitudinal, accelerating component of electric field. Gradients of 100 GV/m have been reached over short distances in laser driven plasma wakefield accelerators, and up to 100 MeV energy gain has been

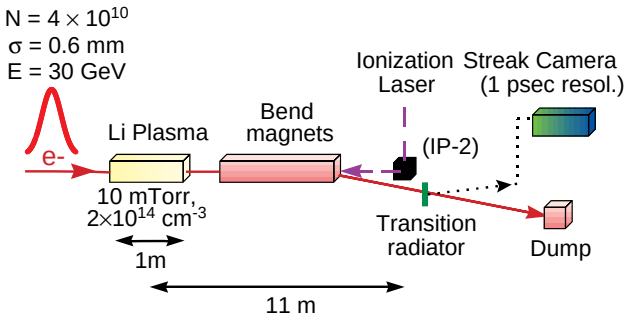

Figure 4: Schematic of E-157, the plasma wakefield acceleration experiment, to be performed in the SLAC Final Focus Test Beam (FFTB).

measured.[9,10] These are impressive accomplishments with the potential of revolutionary changes in particle accelerators.

They have led to controversy also. Some plasma researchers have boldly extrapolated these successes into visions of small, inexpensive colliders capable of doing the particle physics research of larger, conventional accelerators. This is a vision that has attracted attention in the popular press and natural skepticism in the scientific community. That skepticism is based on *i)* the present limited experience and *ii)* the many facets of a high energy collider: beam quality and control and stability, staging of multiple acceleration sections, power source efficiency, etc., that are yet to be considered. Plasma acceleration could be a revolutionary development or it could be as difficult and distant as fusion production of energy has proven to be.

However despite skepticism, the promise and potential of plasma accelerators challenges one to test and explore them in new ways with different implications for possible future applications. SLAC experiment E-157 is such an exploration. The objective is measurement of the behavior of a well-characterized beam in a long plasma with the immediate goal of achieving up to 1 GeV energy gain with a gradient of 1 GeV/m.

The experiment, to be performed by a collaboration of physicists from LBNL, UCLA, USC and SLAC,[11] is illustrated schematically in Figure 4. The plasma is "underdense", the beam density is greater than the plasma density, and plasma electrons along the beam path are expelled by the beam as it passes. The ions are stationary. This creates a high-gradient accelerating structure with a wavelength, λ_p, set by the plasma density, n_0,

$$\lambda_p(\mathrm{mm}) \approx \sqrt{\frac{1}{n_0(10^{15}\,\mathrm{cm}^{-3})}}. \qquad (7)$$

A large accelerating voltage

$$E_z(\mathrm{GV/m}) \approx 3.2\sqrt{n_0(10^{15}\,\mathrm{cm}^{-3})} \qquad (8)$$

is produced after the beam passage as the space charge force from the ions draws the expelled electrons back.

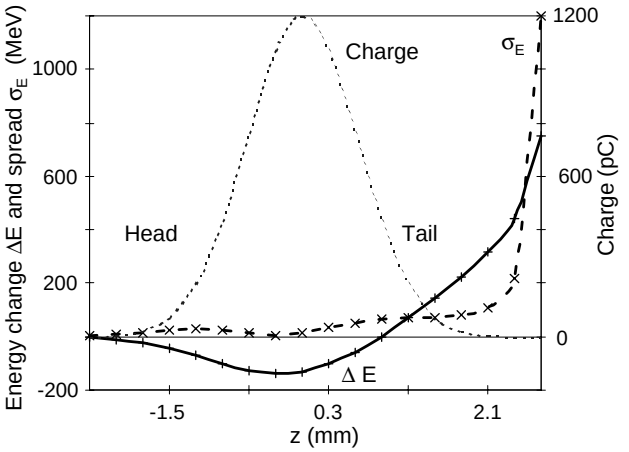

Figure 5: The expected experimental signature; mean change in energy (solid line) and energy spread (dashed line) in 1 psec slices along the beam.

Energy extracted from the head of the beam has created a wakefield that accelerates the tail. The resultant peak accelerating field is ~ 1 GeV/m for the E-157 parameters. Shortening the bunch and increasing the plasma density would dramatically increase the gradient. For example, σ = 0.4 mm and $n_0 = 10^{15}$ cm^{-3} would increase the peak accelerating gradient to ~ 2.5 GeV/m.

The primary diagnostic will be a streak camera with 1 psec resolution in the conditions of this experiment. Acceleration will be measured by measuring the beam deflection in a dispersive region of the FFTB. Figure 5 shows the expected signal; the tail of the beam will have a mean energy increase of ΔE ~ 750 MeV and an RMS energy spread of over 1 GeV.

Not only is the combination of accelerating gradient and length unprecedented, but the focusing fields are also. Once the electrons have been expelled, the remaining ion column forms a uniform focusing field with a gradient of 6000 T/m. It won't be possible to match the beam into this strong lens for two reasons: *one of principle* - the ion column is formed as the head of the beam expels electrons, and the head and tail experience different focusing gradients; and *a practical one* - the matched β and spot size are 12 cm and 4 μm, respectively, and they cannot be achieved with the FFTB magnets. The solution will be to have an integral number of betatron oscillations in the plasma as shown in Figure 6.

The beam plasma interaction has been extensively simulated for the E-157 conditions, but the accelerating and focusing field strengths and the transient nature of the plasma phenomena make unanticipated effects likely. Important advantages for understanding these effects will be the knowledge of the SLC beam and the FFTB optics together with the extensive diagnostics for measuring beam properties including trajectory, β-functions, and emittances. The incoming beam will be well-characterized. Measuring and explaining the properties of the outgoing beam promise to give new insights into the beam-plasma interaction,

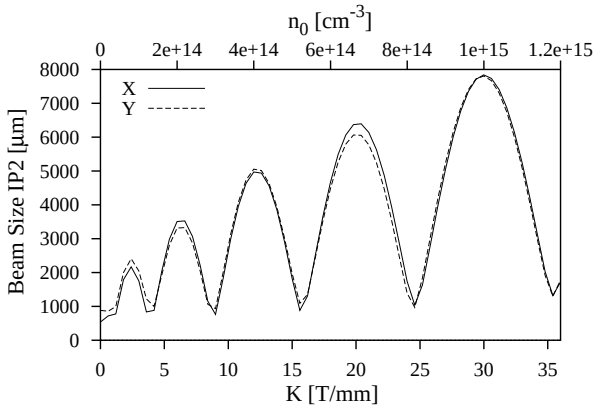

Figure 6: Betatron beam sizes at the diagnostic point (IP2) for different plasma densities.

insights into fundamentals of particle acceleration and the viability of plasma accelerators.

IV. MM-WAVE ACCELERATORS

The predominant experience with RF linacs has been at S-band, but efficiency and gradient limitations argue for shorter wavelengths as the energy increases. The NLC is optimized for E_{CM} ~ 1 TeV and is at X-band. While some aspects of the NLC are scaled from S-band, designing a TeV energy collider has required significant innovations. Still shorter wavelengths and more innovations are going to be necessary for multi-TeV energies.

Our research in short wavelength, high gradient, RF driven acceleration has concentrated on 90 GHz which is in the middle of W-band.[12] It involves understanding of gradient limitations, developing collider concepts consistent with those limitations, application of new technologies to accelerator fabrication, and some preliminary work on W-band power sources. All of this is being done with a short range goal of building a 1 m long, 1 GeV accelerator.

A. Gradient Limitations

P. Wilson has developed convenient parametrizations for gradient limits from trapping of field emitted electrons and from RF breakdown.[13] Field emitted electrons can be accelerated to relativistic energies in a RF cycle and trapped by a traveling RF wave when the gradient exceeds

$$G_{trap} = \frac{\pi mc^2}{\lambda} = \frac{1.6\ \text{MeV}}{\lambda}. \qquad (9)$$

This is not a rigorous bound, but possible deleterious effects from trapped dark current include beam loading, random deflecting wakefields, radiation damage, and backgrounds in diagnostics and, possibly, the high energy physics experiment.

The RF breakdown limit is empirical and is based on experiments of breakdown at fixed pulse length and different frequencies[14] and experiments at different pulse lengths and the same frequency, f = 8.568 GHz.[15]

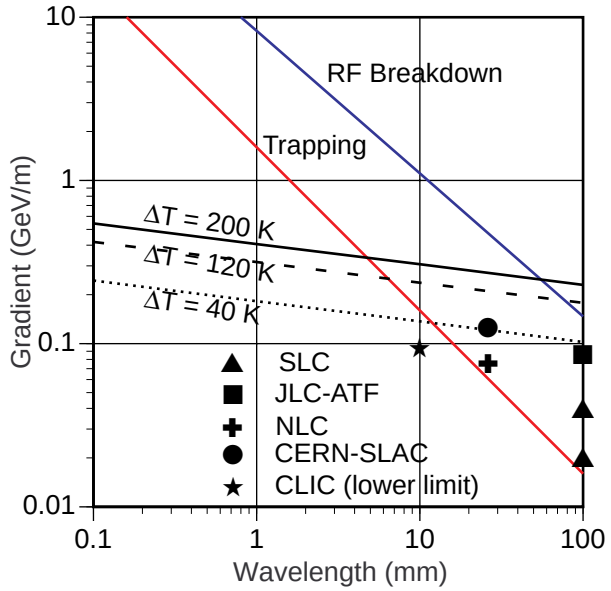

Figure 7: Gradient limits due to dark current trapping, RF breakdown, and pulsed heating. The data points are achieved gradients at different frequencies. Pulsed heating is scaled from NLC as described in text. Data are from SLC, NLC,[16] CERN-SLAC,[17] CLIC,[18] JLC-ATF[19]; they represent gradient achieved with reasonable dark current.

Combining these assuming the same fractional fill time gives[13]

$$G_{break} = \frac{1.1\,\mathrm{GeV/m}}{[\lambda(\mathrm{cm})]^{7/8}}. \qquad (10)$$

This result should be taken as rough guidance only because it is based on only two experiments and because there is little understanding of the underlying causes of RF breakdown.

These two expressions are shown in Figure 7 together with gradients measured at different frequencies. The data and limits are consistent, and trapping is the more restrictive at long wavelengths. Based on considerations of trapping and breakdown only, the wavelength must be in the mm range to reach gradients of ~ 1 GeV/m. However, at that wavelength pulsed heating appears to be more important. This phenomenon needs to be understood, and accommodated in the accelerator design.

B. Pulsed Heating

RF surface currents flow within a few skin depths of the surface. The skin depth of copper at W-band is $\delta \approx 0.2$ μm. The resulting heat diffuses away from the surface with a diffusion depth proportional to the square root of time. For a square pulse of length T_p and gradient G the maximum surface temperature is[13]

$$\Delta T = \frac{G^2\sqrt{T_p}}{Z_H^2}\frac{R_s}{\sqrt{\pi \rho c_\varepsilon k}} \qquad (11)$$

where R_S is the surface resistance, ρ is the density, c_ε is the specific heat, and k is the thermal conductivity. The impedance Z_H is the ratio

$$Z_H = \frac{G}{H_{max}} \qquad (12)$$

where H_{max} is the maximum surface magnetic field. Using NLC values, Z_H = 300 Ω and T_p = 360 nsec, and scaling pulse length with filling time, $T_p \sim \lambda^{3/2}$, gives the pulsed heating curves in Figure 7.

Surface pulsed heating can lead to fatigue and failure of metals. As the surface heats it expands in the unconstrained direction normal to the surface and goes into compression in the tangential direction where it is constrained. Plastic deformation occurs when the compression exceeds the yield strength. This corresponds to a temperature rise

$$\Delta T_y = \frac{(1-\nu)Y}{E\alpha} \qquad (13)$$

where ν is Poisson's ratio, Y is the yield strength, E is Young's modulus, and α is the coefficient of linear expansion.

Repeated cycling results in the formation of slip bands and fatigue cracks, but the temperature rise that causes this damage is a factor above ΔT_y. There is disagreement over both the numerical value of this factor and the physical origin of it. For copper ΔT_y = 22K,[20] and estimates for the damage threshold include ΔT = 40K[21] and ΔT = 110K.[22] Once the threshold is exceeded, the lifetime of the metal, N_τ measured in cycles, is exponential in the stress amplitude, σ, with a scale factor σ_S[22,23]

$$N_\tau \propto \exp(-\sigma/\sigma_S). \qquad (14)$$

The tolerable pulsed temperature rise in RF systems is critical for determining the achievable gradient at short wavelengths, and a series of experiments designed to measure it has begun. The experimental goals are:

- To measure the damage threshold for copper and other materials including composites and materials with surface coatings. For example, dispersion strengthened copper, Glidcop AL-15, has ΔT_y = 120K.[24]
- To verify the exponential relationship between lifetime and stress amplitude.
- To establish the scale factor σ_S in eq. (14). Kovalenko has developed a model where σ_S depends on the evaporation energy and on ambient temperature.[22]

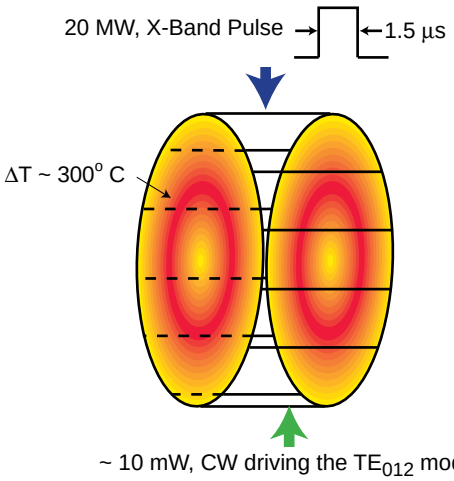

Figure 8: Schematic of pulsed heating experiment.

The experiment is illustrated in Figure 8. A TE_{011} mode in an X-band pill-box cavity is driven by a 20 MW, 1.5 μsec long, 60 Hz repetition rate RF pulse.[25] The surface current on the endcaps follows a J_1 Bessel function, and the pulsed temperature rise at the center of the endcaps can be up to $\Delta T \sim 300K$. Temperature rise is measured by changes in reflection of the TE_{012} mode that is excited with low power CW RF. The endcaps can be removed for metallurgical examination after an exposure.

The first round of this experiment has been performed with over 10^7 pulses on copper endcaps with $\Delta T > 100K$. There was no degradation of the Q's of the TE_{011} or TE_{012} modes, but there was some evidence of changes in crystal structure at the RF surface.[26] The experiment is currently being redesigned to eliminate problems with RF breakdown and the diagnostic RF signal, and it is expected to be running again with higher temperature rises in Spring, 1998.

C. Wakefields

Wakefields depend strongly on wavelength, for example

$$W_{\perp,\text{effective}} \propto \frac{1}{\lambda^3}, \qquad (15)$$

and wakefield effects in a mm-wave accelerator must managed with a combination of reducing the accelerated charge and precise alignment. The next section deals with the former and this section with the latter.

Recent experiments have demonstrated high precision, beam based alignment using accelerator structures themselves as beam position detectors.[27] The experiments were performed at the ASSET facility located in the SLAC linac after the SLC damping rings and shown in Figure 9.[28] Electron and positron beams from the damping rings are launched on parallel trajectories The positron intensity is substantially higher, and the positron beam transverse wakefields are measured by means of the trajectory of the weaker electron beam. Both short- and long-range

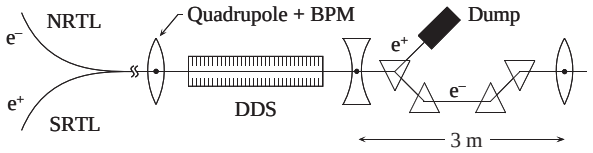

Figure 9: The ASSET facility.[28]

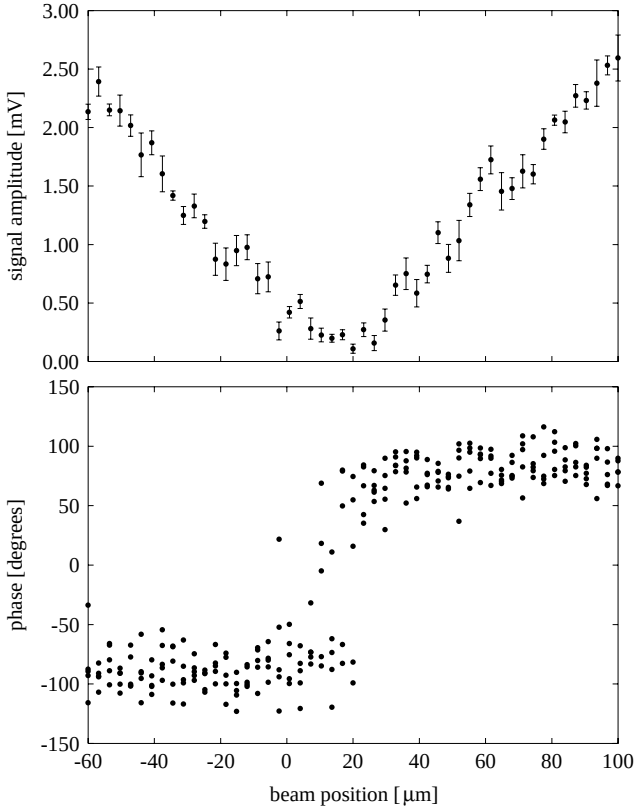

Figure 10: Amplitude and phase of the dipole mode signal at f = 14.9675 GHz.[30]

wakefields can be measured by varying the time between the beams.

The transverse wakefields of a 1.8 m long, X-band damped-detuned structure (DDS)[29] were measured. The DDS has RF manifolds for damping the lowest frequency deflecting mode in a band centered at 15.1 GHz. These manifolds have windows for either attaching external loads or measuring the beam induced signal. The amplitude and phase of one dipole mode is shown in Figure 10. The amplitude has a minimum and the phase changes by 180° in a region that is ± 10 μm wide which was comparable to the beam jitter.

The beam was centered at both ends of the DDS structure using these single mode signals, and then the short-range wakefield, which depends on many modes, was measured with the electron beam. This second measurement showed that the beam was centered to ± 25 μm. Understanding and improving this resolution will require further experiments.

The central feature tested in this experiment was that deflecting mode signals can be used to directly measure

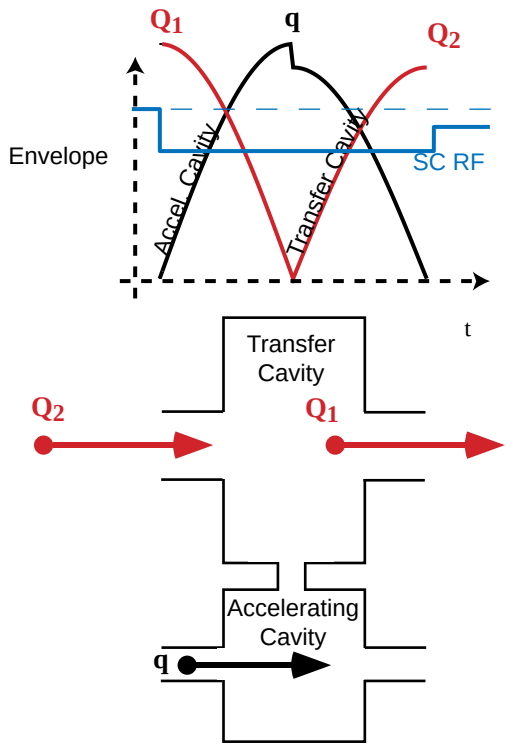

Figure 11: The field envelopes and accelerator configuration of the cavity beat-wave accelerator concept.

the relative alignment of beam and accelerator. This technique could be generalized to using deflecting mode signals in feedback loops that would move structures to maintain alignment. Such ideas will be critical for wakefield control in a mm-wave accelerator.

D. Collider Configurations

The relationship between luminosity, L, single beam power, P_B, center-of-mass energy, E_{CM}, vertical spot size, σ_y, and experimental backgrounds measured by the number of beamstrahlung photons per incident particle, n_γ, is

$$L = \frac{1}{4\pi\alpha r_e}\frac{n_\gamma}{E_{CM}}\frac{P_B}{\sigma_y}. \qquad (16)$$

High luminosity requires a small beam spot and large beam power, and these require small emittance and good acceleration efficiency, respectively. This is accomplished in the NLC design with relatively low charge per bunch and multiple bunches per RF pulse.

This multiple bunch strategy cannot be followed to $\lambda \sim 1$ mm. Wakefields and emittance preservation favor small charge per bunch and a large number of bunches, but pulsed heating argues for a short RF pulse. Pulsed temperature rise $\Delta T = 200$ K might be possible, but even in that case the gradient limit would be $G < 0.5$ GeV/m if the pulse length scaled as assumed in Figure 7. Higher gradient requires a shorter RF pulse. Satisfying the constraints of a high energy collider will need qualitative changes in accelerator configuration.

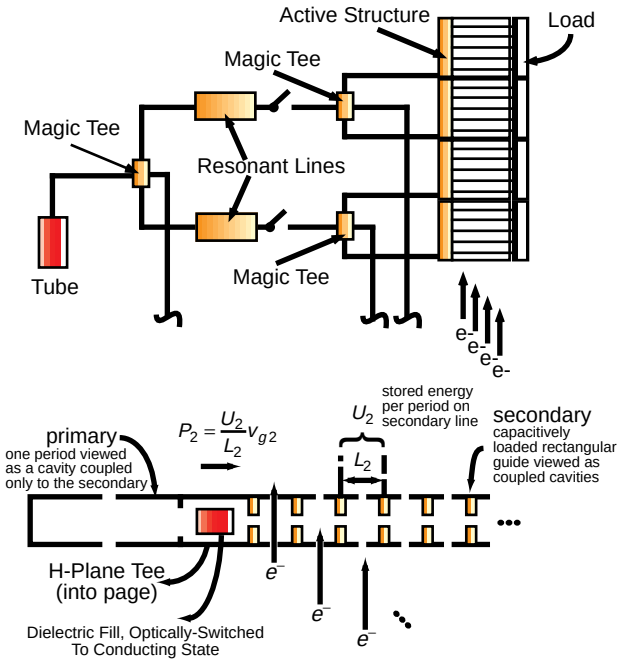

Figure 12: The matrix accelerator.

There are two ideas that have been considered. The first is the "cavity beat-wave accelerator"[31] which is a two-beam accelerator with energy recovery illustrated in Figure 11. High charge bunches Q_1 and Q_2 pass through a mm-wave cavity, the transfer cavity. The first bunch, Q_1, excites the fundamental mode of the transfer cavity. The accelerating cavity fundamental frequency is close to that of the transfer cavity, and energy beats between the transfer and accelerating cavities. The high energy beam, q, is accelerated during the first of these beats. Drive bunch Q_2 passes through the transfer cavity the first time the energy reappears there, and it is phased such that energy is extracted from the cavity fields. The drive beam is accelerated by a superconducting RF cavity. The bunches are spaced appropriately such that Q1 extracts energy from the superconducting cavity and Q2 restores energy. The net energy loss from the superconducting RF is the energy transferred to bunch q and due to inefficiencies.

The cavity beat wave accelerator has been analyzed for mm-waves and 1 GeV/m gradient.[32] The drive beam charge was 110 nC, and transverse stability of the drive beam would require strong focusing that could possibly be obtained with exotic techniques like ion-channel guiding.[33] The key to further development is solving the drive beam transverse dynamics.

The "switched matrix accelerator", illustrated in Figure 12, is a more radical idea.[8] The RF and beams travel in perpendicular rather than parallel directions. The gradient part of the structure is exposed to RF for a short time, thereby limiting the pulsed heating, and yet the RF efficiency is high because multiple beams are accelerated.

The first element is an RF power source with a relatively long pulse that is compressed to approximately

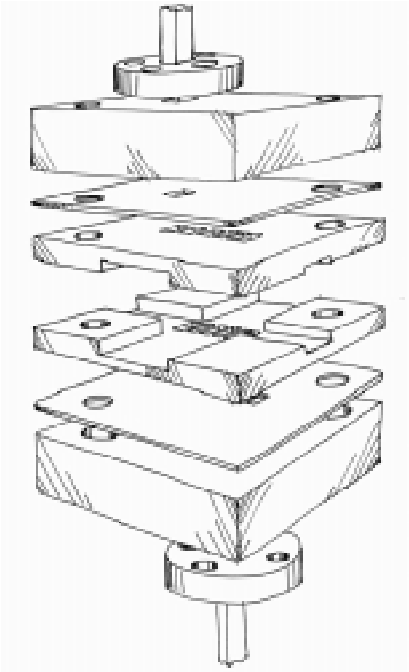

Figure 13: Sketch of the first SLAC mm-wave accelerator structure. The top and bottom layers provide mechanical strength and taper from WR10 waveguide. The thin intermediate layers contain the coupling irises. The middle layer, one piece split in two in this picture for purposes of illustration, contains the beam and vacuum pipes and the seven cells.

200 MW, 10 ns long pulses. This power is distributed to the primary transmission lines of the accelerator which are then discharged in sub-nanosecond pulses into secondary lines where the beams are accelerated. The beams must combined after acceleration most likely through a non-isochronous beam transport.

At the present time D. Whittum is calculating properties of matrix accelerator with concentration on the primary and secondary transmission lines such that there is good energy efficiency and low dispersion of pulses in the secondary lines. There are important technological issues in addition to these considerations. They are the mm-wave power source, the pulse compressor, and the switches that discharge the primary into the secondary transmission lines. There are ideas and/or the beginnings of work in all these areas:

- A multi-hundred kW klystron array is being designed that is based on permanent magnet focusing, quasi-optical combining of power, and the fabrication methods discussed in the next section.[34] While not adequate for a collider RF power source, this klystron would produce record power at W-band and be the beginning of high power mm-wave production at SLAC.
- The klystron is serving as an introduction to quasi-optical techniques which are certain to be necessary for high power W-band RF manipulations.

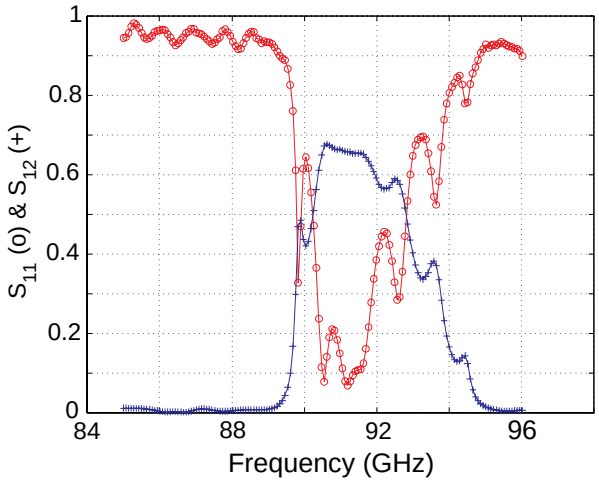

Figure 14: Reflection (S_{11}) and transmission (S_{12}) measurements.

- There has been a first test of an optically triggered silicon RF switch, and active pulse compression has been demonstrated at moderate power.[35]

The underlying idea of the matrix accelerator, orthogonal propagation of beam and RF power, has the potential for the efficient use of short, high power pulses. It appeared in the laser driven accelerator for the same reason The idea's merit for mm-waves depends on the calculations described above, and it depends on recombining wavefronts in the laser accelerator case. In both cases there is the need for successful development of the required technologies also.

E. MM-Wave Accelerator Fabrication

MM-wave accelerators have mm feature sizes, and scaling from S- and X-band accelerators and from numerical models the dimensional tolerances are 2 - 5 μm on critical features. These feature sizes and tolerances suggest fabrication by LIGA where a plastic mold is made by exposure to high energy X-rays.[36] This is followed by chemical removal of radiation damaged plastic and electrodeposition of metal into the mold to produce the final part.

We have not pursued LIGA because: *i)* reducing the consequences of pulsed heating could require materials such as Glidcop that cannot be electrodeposited, and *ii*) the large initial investment to gain proficiency with LIGA. Wire EDM (ElectroDischarge Machining) routinely reaches better than 5 μm level of precision,[37,38] and EDM machines with sub-micron precision are being manufactured although they are not readily available.

A planar,[39] seven-cell, 2π/3 traveling wave structure, illustrated in Figure 13, was designed, machined using wire EDM by Ron Witherspoon, Inc., and measured.[37,40] The reflection and transmission were measured and are shown in Figure 14. These results had both encouraging and discouraging aspects. The encouraging ones were that a

structure could be fabricated with wire EDM techniques and the mode pattern was close to that expected.

The discouraging aspect was that the peak transmission was less than 70% when roughly 95% was expected. The possible contribution of surface finish to losses was measured in a separate experiment using two-inch long WR10 waveguides machined with wire EDM. It was found that with the 0.2 μm rms finish of the seven-cell structure the effective conductivity was $\sigma = 2.5\times10^7$ Ω/m as compared to $\sigma = 6.0\times10^7$ Ω/m for OFE copper.[41] This is not enough to account for the low transmission. Other experiments eliminated energy propagation out of the beam or vacuum ports. This leaves the contact between the layers, which were just clamped together, as the most likely explanation. The next structure will be diffusion bonded to eliminate this cause of energy loss.

This next structure will have twenty-five cells and will also include a number of design innovations including compatibility with vacuum pumping and water cooling and having all of the machining including waveguide tapers and coupling irises in a single layer.[37] Machining is expected to be complete in early 1998, and we are looking forward to measuring its properties.

Once that is completed there are plans to place it or a similar structure in the NLC Test Accelerator beam and use that beam to generate RF power in a test of a high power mm-wave accelerator. This will be the first opportunity to see if the extrapolation of gradient limit from RF breakdown (Figure 7) has some validity.

V. CONCLUDING REMARKS

The SLAC advanced accelerator program described in this paper is an attempt to pose and answer questions that could lead to inventions or dramatic changes in electron linear accelerators. All of the work described is speculative, but, hopefully, well motivated and focused on significant problems.

SLAC ARDB (Accelerator Research Department B) is at the center of this work and has been fortunate to have strong support from the laboratory and enthusiastic collaboration within SLAC, other academic institutions, and industry.

VI. FOOTNOTES & REFERENCES

1. M. D. Perry, AIP Conf. Proc. 335, 75 (1995).
2. Y. C. Huang *et al*, Applied Physics Letters **68**, 753 (1996).
3. L. W. Davis, Physical Review A **19**, 1177 (1979).
4. Y. C. Huang and R. L. Byer, Applied Physics Letters **69**, 2175 (1996).
5. T. Plettner, private communication.
6. Laser Acceleration Collaboration: R. L. Byer, R. H. Pantell, T. Plettner, Y. C. Huang (Ginzton Laboratory); R. L. Swent, T. I. Smith (Hansen Laboratory); J. E. Spencer, R. H. Siemann, H. Wiedemann (SLAC).
7. R. L. Byer, private communication.
8. D. H. Whittum, SLAC technical note ARDB-086.
9. A. Modena et al, Nature **337**, 606 (1995).
10. K. Nakajima et al, AIP Conf Proc **398**, 83 (1997).
11. E-157 Collaboration: S. Chattopadhyay, W. Leemans (LBNL); C. Clayton, C. Joshi, K. Marsh, W. Mori, G. Wang (UCLA); T. Katsouleas, S. Lee (USC); R. Assmann, P. Chen, F. J. Decker, R. Iverson, P. Raimondi, T. Raubenheimer, S. Rokni, R. Siemann, D. Walz, D. Whittum (SLAC).
12. This W-band research is a collaboration of SLAC Accelerator Research Department B (ARDB), other SLAC departments, and collaborators from other institutions: T. Chen, P. J. Chou, M. Hill, T. Knight, X. Lin, A. Menegat, D. Palmer, B. Podobedov, D. Pritzkau, M. Seidel, A. Seymour, R. Siemann, J. Spencer, D. Whittum, X. Xu (SLAC ARDB); C. Adolphsen, G. Bowden, R. Carr, G. Caryotakis, M. Copeland, A. Farvid, R. Folkes, R. Kirby, K. Ko, N. Kroll, R. Loewen, E. Lundahl, R. Miller, C.-K. Ng, A. Odian, C. Pearson, M. Petelin, R. Phillips, R. Pitthan, G. Scheitrum, Y.-Y. Sung, A. Vleiks, C. Yoneda, P. Wilson (other SLAC departments); W. Bruns, H. Henke, R. Merte (Tech. Univ. Berlin); T. Lee, D. Yu (DULY Research); D. Miller (EMT); S. Schultz (Univ. of Cal, San Diego): S. Schwartzkopf, R. Witherspoon (Ron Witherspoon, Inc.).
13. P. B. Wilson, AIP Conf Proc **397**, 191 (1997).
14. G. A. Loew and J. Wang, SLAC-PUB-4647.
15. A. Vlieks *et al*, SLAC-PUB-4546.
16. J. W. Wang *et al*, Proc of 17th Int. Linac Conf, 305 (1994).
17. J. W. Wang *et al*, Proc of 18th Int. Linac Conf, (Geneva, 1996).
18. R. Bossart *et al*, Proc of 1994 European Accel Conf., 680 (1994).
19. H. Matsumoto, Proc of 18th Int. Linac Conf, (Geneva, 1996).
20. Based on $Y = 6.9\times10^7$ N/m^2, $E = 1.17\times10^{11}$ N/m^2, $\alpha = 1.73\times10^{-5}$, and $\nu = 0.345$.
21. H. M. Musal, Jr, Laser Induced Damage in Optical Materials 1979, Nat Bureau Standards Spec Pub 568, 159 (1980).
22. V. F. Kovalenko, Physics of Heat Transfer and Electro-Vacuum Devices, Sovetskoe Radio (1975).
23. A. Weronski and T. Hejwowski, Thermal Fatigue of Metals, Marcel Dekker, Inc. (New York, 1991).
24. SCM Metal products, Inc., Cleveland, Ohio. ΔT_y based on $Y = 35\times10^7$ N/m^2, $E = 1.15\times10^{11}$ N/m^2, $\alpha = 1.66\times10^{-5}$, and $\nu = 0.35$.

25. D. Pritzkau *et al*, presented at 1997 Part. Accel. Conf.
26. D. Pritzkau, private communication.
27. M. Seidel *et al*, submitted to Nucl. Inst. & Methods.
28. C. Adolphsen *et al*, Phys Rev Lett **74**, 2475 (1994).
29. N. Kroll *et al*, presented at the 1997 Part. Accel. Conf.
30. M. Seidel, presented at the 1997 Part. Accel. Conf.
31. H. Henke, CERN-LEP-RF/88-55.
32. D. H. Whittum *et al*, submitted to 1997 Part Accel Conf.
33. D. H. Whittum *et al*, Phys. Rev. **A** 6684 (1992).
34. G. Caryotakis *et al*, SLAC-PUB-7624 (1997).
35. S. Tantawi *et al*, SLAC-PUB-7368 (1996).
36. E. W. Becker *et al*, Microelectronic Engineering **4**, 35 (1986). LIGA is an acronym for Lithografie, Galvanoformung and Abformung.
37. P. J. Chou *et al*, SLAC-PUB-7498, submitted to 1997 Part Accel Conf.
38. In a seven-cell test performed on an Agiecut 150 HSS deviation of nominal centers of cavities was within 1 μm, and the variation in sizes was less than 2.7 mm. Ref [37].
39. LIGA and wire EDM favor a planar structures, and, in addition, the matrix accelerator is most natural planar geometry.
40. P. J. Chou *et al*, SLAC-PUB-7499, submitted to 1997 Part Accel Conf.
41. For comparison, 1.5 μm rms surface finish had an effective conductivity of $\sigma = 6.3\times10^6\ \Omega$/m, and when chemically etched this could be increased to $\sigma = 4\times10^7\ \Omega$/m